J Mater Sci (2011) 46:7737–7744
DOI 10.1007/s10853-011-5753-8

Influence of heat treatments on toughness and sensitization of a Ti-alloyed supermartensitic stainless steel

G. F. da Silva · S. S. M. Tavares · J. M. Pardal · M. R. Silva · H. F. G. de Abreu

Received: 7 April 2011 / Accepted: 26 June 2011 / Published online: 9 July 2011
© Springer Science+Business Media, LLC 2011

Abstract Supermartensitic steels are a new class of martensitic stainless steels developed to obtain higher corrosion resistance and better toughness through the reduction of carbon content, and addition of Ni and Mo. They were developed to more critical applications or to improve the performance obtained with conventional grades AISI 410, 420, and 431. In this study, the influences of the tempering parameters on the microstructure, mechanical properties (hardness and toughness), and sensitization of a Ti-alloyed supermartensitc stainless steel were investigated. The material showed temper embrittlement in the 400–600 °C range, as detected by low temperature (−46 °C) impact tests. The degree of sensitization measured by double loop reactivation potentiodynamic tests increased continuously with the increase of tempering temperature above 400 °C. Healing due to Cr diffusion at high tempering temperatures was not observed. Double tempered specimens showed high amounts (>20%) of reverse austenite but their toughness were similar to specimens single tempered at 625 and 650 °C.

G. F. da Silva
PETROBRAS-UO-Rio, Rua General Canabarro, 500, Rio de Janeiro CEP 20271-205, Brazil

S. S. M. Tavares (✉) · J. M. Pardal
Departamento de Engenharia Mecânica, Universidade Federal Fluminense, Rua Passo da Pátria, 156, Niterói CEP 24210-240, Brazil
e-mail: ssmtavares@terra.com.br

M. R. Silva
Instituto de Ciências, Universidade Federal de Itajubá, Minas Gerais, Brazil

H. F. G. de Abreu
Departamento de Engenharia Metalúrgica e Materiais, Universidade Federal do Ceará, Campus do Pici, Bloco 702, Fortaleza CEP 60455-760, Brazil

Introduction

Supermartensitic stainless steels (SMSS) are a new generation of 12–13%Cr martensitic steels, with very low carbon (<0.03%) and additional alloying of nickel and molybdenum [1]. Titanium and/or niobium can also be added in order to improve the intergranular corrosion resistance and mechanical properties [2–4]. As a result, the new SMSS have better corrosion resistance, weldability and low temperature toughness than conventional 12–13%Cr martensitic grades (AISI 410 and AISI 420). Despite of the low carbon contents, SMSS also present high mechanical strength levels when compared to austenitic, ferritic, and duplex grades, due to the tempered martensitic structure.

Martensitic stainless steels are usually oil quenched and tempered. In conventional grades, care must be taken to choose the tempering temperature. Intermediate tempering temperatures must be avoided due to temper embrittlement and corrosion resistance decay [5–8]. For instance, Čihal and Štefec [7] found that a 15Cr17Ni2 martensitic steel was sensitized by tempering between 450 and 650 °C. AISI 410 undergoes embrittlement and has the corrosion resistance decreased between 370 and 650 °C [6].

Sensitization is usually defined as intergranular chromium carbide precipitation which causes Cr depletion in the vicinity of grain boundaries. As a consequence, the steel becomes susceptible to intergranular corrosion when submitted to aggressive environments, with the Cr-depleted areas showing an anodic behavior.

These Cr-depleted regions present a weakest passive layer, with an anodic behavior in front of the unaffected

zones. The steel becomes susceptible to intergranular corrosion when submitted to aggressive environments.

Nickel–chromium martensitic steels are particularly prone to temper embrittlement when tempering is performed in the interval of 350 and 570 °C or during slow cooling through this range. Temper embrittlement can be detected by traditional impact tests, and is usually attributed to traces of impurities, such as sulfur, phosphorus, antimony, arsenic, and tin [9]. According to the API Recommended Practice 571 [10] equipments made of temper embrittled materials may present catastrophic failure during start up and shutdown.

The purpose of this study was to investigate how the microstructure, toughness, hardness, and intergranular corrosion susceptibility of a novel supermartensitic stainless steel are influenced by the tempering heat treatment.

Experimental

Specimens from a supermartensitic stainless steel containing 0.0278%C–12.21%Cr–5.8%Ni–1.95%Mo–0.52%Mn–0.28%Ti–0.0112%P–0.0019%S–0.013%N (wt%) were cut and machined to the dimensions of sub-size Charpy impact test specimens ($55 \times 10 \times 7.5$ mm^3) and corrosion test specimens ($10 \times 10 \times 4$ mm^3). The specimens were oil quenched after soaking at 1000 °C for 1 h. After this the specimens were tempered at different temperatures. Two double tempering treatments were also carried out. Table 1 gives the details of tempering treatments and informs the specimens identification used in this study.

The susceptibility to intergranular corrosion was evaluated by double loop electrochemical potentiodynamic reactivation tests (DL-EPR) [11, 12]. These tests were carried out in a conventional three cell electrode assembled with working electrode, Pt foil as auxiliary electrode, and saturated calomel electrode (SCE) as reference. The working electrode was constructed using the supermartensitic steel specimens embedded in epoxy resin with a cooper wire for electric contact. They were ground with 400 emery paper, degreased with alcohol and cleaned in water. The tests were controlled by a μ-AUTOLAB potentiostat–galvanostat, starting with the stabilization of the open circuit potential (E_{OCP}). The potential was then increased in the anodic direction at 1 mV s^{-1} up to the potential of 0.3 V_{SCE}. Then, the scan was reversed, maintaining the same sweeping rate in the cathodic direction. The loss of corrosion resistance was measured by the ratio I_r/I_a, also known as degree of sensitization (DOS), where I_a is the activation peak current of the anodic scan, and I_r is the reactivation peak current observed in the reversed scan.

Table 1 Specimens identification and heat treatments of specimens for mechanical tests (impact and hardness) and DL-EPR tests

Identification	Heat treatment
Q	Oil quenched from 1000 °C
QT-300	Quenched and tempered at 300 °C for 1 h
QT-400	Quenched and tempered at 400 °C for 1 h
QT-500	Quenched and tempered at 500 °C for 1 h
QT-550	Quenched and tempered at 550 °C for 1 h
QT-575	Quenched and tempered at 575 °C for 1 h
QT-600	Quenched and tempered at 600 °C for 1 h
QT-625	Quenched and tempered at 625 °C for 1 h
QT-650	Quenched and tempered at 650 °C for 1 h
Q-DT1	Quenched and double tempered (670 + 600 °C/2 h)
Q-DT2	Quenched and double tempered (670 + 600 °C/8 h)

The DL-EPR test was initially developed for austenitic AISI 304 steels [12] using a 0.5 mol L^{-1} H_2SO_4 + 0.01 mol L^{-1} KSCN solution as the electrolyte. The test may be applied to other types of stainless steels, but modifications in the original solution may be necessary.

Two electrolytes were tested to evaluate the supermartensitic steel in this work. Solution 1 is the standard solution used for austenitic AISI 304 steel (0.5 mol L^{-1} H_2SO_4 + 0.01 mol L^{-1} KSCN). Solution 2 is a less aggressive solution composed of 0.25 mol L^{-1} H_2SO_4 + 0.01 mol L^{-1} KSCN.

The Charpy impact tests were carried out at room temperature (22 °C) and −46 °C in a Heckrt Veb Werk Stoffpruf OS30-300L with capacity of 300 J. Three specimens per condition were tested and the average values were presented in the results. After testing some fracture surfaces were observed in the scanning electron microscope (SEM). Hardness tests with load of 30 kgf were also performed in all conditions. Ten tests per condition were performed. Errors bars from hardness and toughness points were determined from standard deviation of measurements.

Microstructural analysis was performed by SEM and magnetic measurements. SEM analyses were performed in ZEISS EVO 40 and JEOL 6510A microscopes, both equipped with energy dispersive spectrometer (EDS). The specimens for SEM analysis were prepared with Vilela's etching (10 mL HCl + 90 mL H_2O + 1 g of picric acid).

A quantitative analysis of the austenite content in the microstructure was performed by magnetic measurements, using the method described by Cullity [13]. Since austenite is paramagnetic and martensite is ferromagnetic, the austenite volume fraction (C_γ) is calculated by the equations:

$$C_M = \frac{m_S}{m_{S(i)}} \quad (1)$$

$$C_\gamma = 1 - C_M \quad (2)$$

where C_M is the martensite volume fraction, m_S is the magnetization saturation of the specimen, and $m_{S(i)}$ is the intrinsic magnetization saturation of the ferromagnetic

phase (martensite). The magnetizations curves to obtain the m_s values were constructed in a vibrating sample magnetometer Lakeshore model 7400, with specimens carefully machined and cut as discs with 3.5 mm of diameter. The magnetization saturation was obtained with an applied field of 1.4 T.

Results and discussion

Figure 1a and b shows the microstructure of the material in the as quenched condition. The large and square shape particles of Fig. 1a were identified by EDS as titanium nitrides (TiN). These particles, which are commonly found in Ti-stabilized stainless steels, were also found in all tempered specimens.

Figure 1b shows small particles in the massive martensitic structure. Although these fine precipitates could not be analyzed by EDS, particles with the same shape and morphology were reported as titanium carbides in a previous work from Rodrigues et al. [4]. According to these authors the excellent mechanical properties of SMSS are mainly attributed to this fine precipitation of titanium carbides.

Figure 2a and b compares the DL-EPR curves of the supermartensitic steel in the as quenched condition (specimen "Q") tested with solutions 1 and 2, respectively. It is expected that the best corrosion resistance of martensitic and supermartensitic stainless steels is attained in the as quenched condition because the maximum amount of Cr is dissolved in the fresh martensite. However, a small reactivation peak is observed in the specimen "Q" when tested with solution 1, but not with solution 2. For this reason, the use of solution 2 seems to be more adequate for the study of influence of tempering on the corrosion resistance of SMSS. Figure 3a and b shows the DL-EPR curves of specimens QT-625 and DT2 tested with solution 2. The DL-EPR curves of double tempered specimens present two activation and two reactivation peaks, reflecting a microstructural change which will be explained later.

Figure 4 shows the evolution of the degree of sensitization (DOS $= I_r/I_a$) with the tempering temperature. The DOS values with solution 1 are significantly higher, as expected. From the data obtained with solution 2, it is possible to affirm that the material becomes sensitized with tempering above 400 °C. The DOS increases continuously with the tempering temperature in the 400–650 °C range, reaching 0.4 in the material tempered at 650 °C and tested with solution 2.

Figure 5 shows the variation of hardness and impact toughness at 22 °C with tempering temperature. A decrease of toughness is observed in specimens tempered at 400 and 500 °C, showing a slight temper embrittlement effect. The material also shows an increase of hardness with the increase of tempering temperature from 300 to 500 °C, which can be attributed to the effect of Mo. As reported by Pickering [5], molybdenum may precipitate as fine $Mo_2(C,N)$ particles during tempering in the 500–550 °C range. Such a fine precipitates were not observed by SEM analysis in this study, but the secondary hardening is clearly seen in Fig. 5.

In Fig. 5, the minimum toughness is coincident with the maximum hardness value, as also observed by Pickering [5] in conventional martensitic stainless steels.

Despite of the similarities with traditional 12%Cr steels, the supermartensitic analyzed in this study presents much higher room temperature toughness than conventional grades AISI 410, 420, and 431 stainless steels, in all tempered conditions. For instance, an AISI 431 steel shows impact energies varying from 10 to 40 J depending on the tempering temperature [14]. It should also be taken into account that the results of impact energy obtained in this work are from sub-size specimens ($55 \times 10 \times 7.5$ mm^3), which means that in a comparison with standard size specimens the SMSS would show a higher superiority. Another important feature is that the fracture analysis of specimens tested at 22 °C showed ductile patterns in all conditions investigated. Figure 6 shows the fracture surface of specimen QT-500, with microvoids and without intergranular cracks and/or cleavage areas.

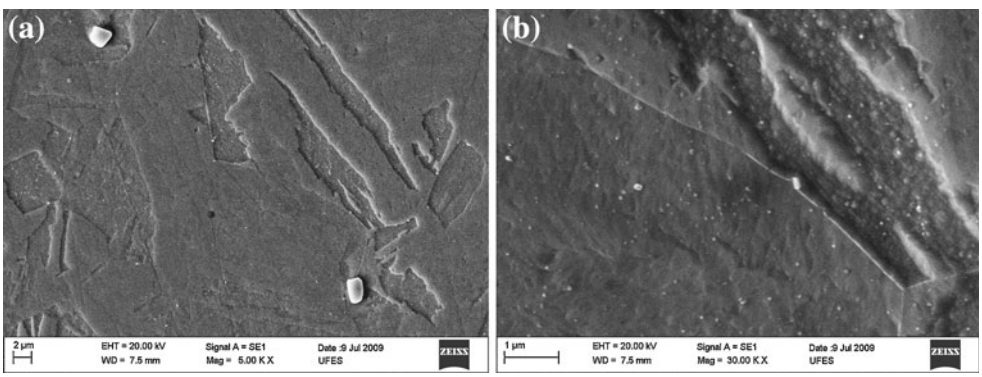

Fig. 1 Microstructure of specimen Q (quenched from 1000 °C)

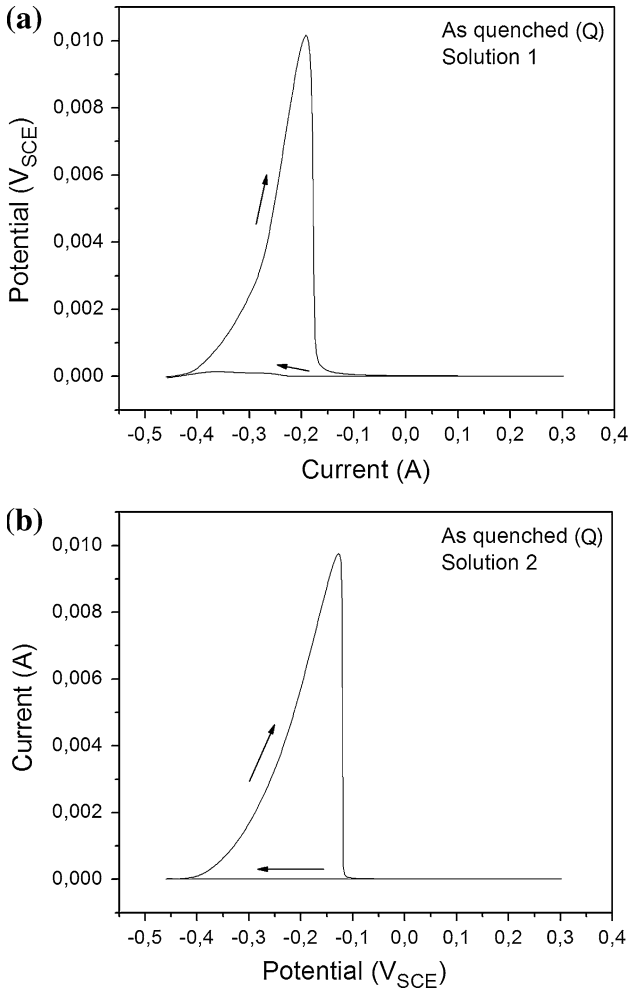

Fig. 2 DL-EPR curves of specimen Q with **a** solution 1 and **b** solution 2

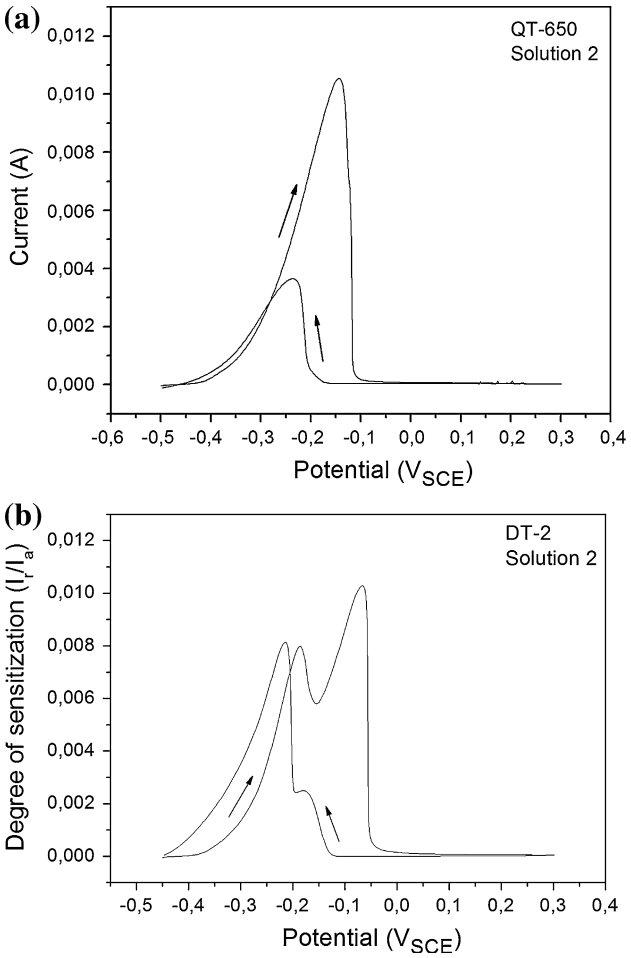

Fig. 3 DL-EPR curves with solution 2: **a** specimen QT 650; **b** specimen DT-2

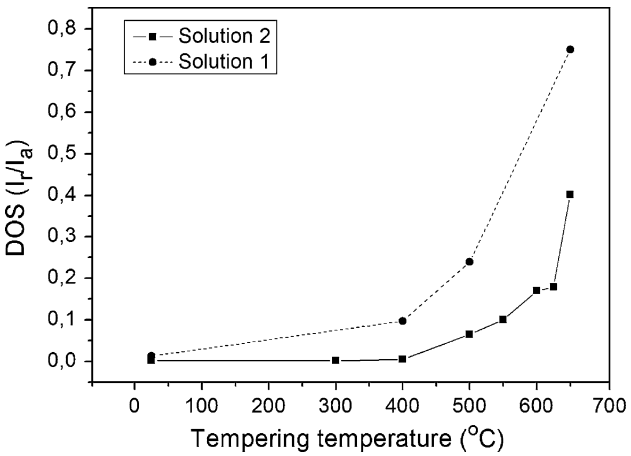

Fig. 4 Variation of the DOS with tempering temperature for tests with solutions 1 and 2

The properties obtained in double tempered specimens DT-1 and DT-2 are shown in Table 2. The toughness values at room temperature tests have the same magnitude of those measured in specimens QT-600, QT-625, and QT-650, and the hardness is similar to QT-650. However, the DOS measured with DL-EPR tests are much higher in the double tempered specimens than in specimen QT-650. It should be expected that the increase of tempering time and temperature above 600 °C would enhance the chromium diffusion and promote a healing effect [5, 7]. Instead, an increase of DOS was measured when the tempering temperature was raised from 600 to 625 and 650 °C, and a further increase was observed in double tempered specimens. Figure 7 shows the specimen DT-1 observed in the light optical microscope just after the DL-EPR with the intergranular attack clearly shown. Similar results were found in a 17-4PH steel with 0.04 wt%C and 0.28 wt%Nb [15].

The A_{c1} temperature for the steel composition calculated with MAP_STEEL_AC1TEMP software [16] was 607 °C. Figure 8 shows the variation of m_S with tempering temperature. An abrupt decrease of m_S is observed with the increase of tempering temperature from 600 to 625 °C,

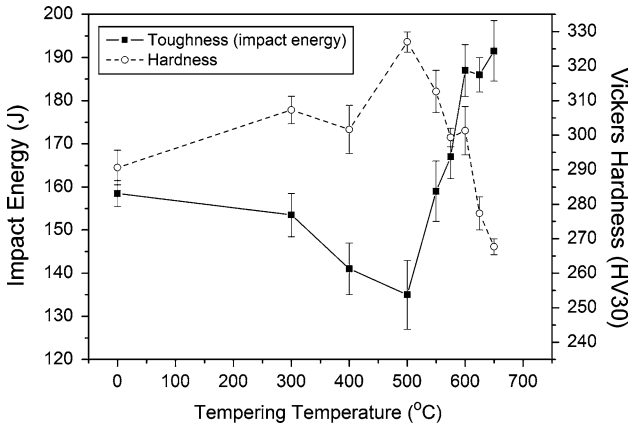

Fig. 5 Variation of hardness and impact toughness at 22 °C with tempering temperature

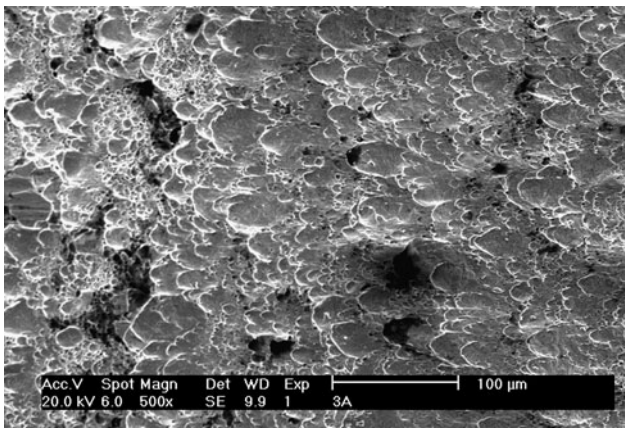

Fig. 6 Surface fracture of specimen QT-500 tested at room temperature

Table 2 Properties of double tempered specimens DT-1 and DT-2

Specimen	Impact energy (J)		Hardness (HV)	DOS (DL-EPR) solution 2
	22 °C	−46 °C		
DT-1	188 ± 6	146 ± 5	270 ± 8	0.80
DT-2	192 ± 6	154 ± 6	261 ± 6	0.76

denoting that the formation of reversed austenite starts in this interval of temperatures, which is in agreement with the A_{c1} prediction. The m_S values of double tempered specimens DT-1 and DT-2 were still lower, 124 and 126 A m^2 kg^{-1}, respectively, which indicates that these samples contain austenite fractions much higher than specimens QT-625 and QT-650. Figure 9 shows the microstructure of specimen DT-1 as observed by SEM. The austenite phase appears as precipitated platelets between the martensite laths, as described by Gesnouin [17] and Bilmes [18].

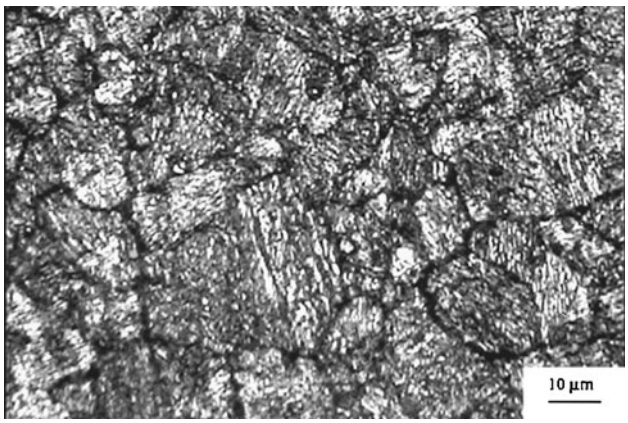

Fig. 7 Specimen DT-1 observed after the DL-EPR test

The amounts of austenite for each heat treatment condition estimated by Eqs. 1 and 2 are shown in Table 3. The $m_{S(i)}$ value was that of the specimen tempered at 400 °C, condition at which the microstructure was 100% martensitic. The as quenched specimen contained a small amount of retained austenite ($C_\gamma = 0.02$ or 2%) which has decomposed during low temperature tempering.

Specimens QT-625 and QT-650 presented austenite fractions 0.12 and 0.09, respectively. The behavior of the amount of reversed austenite at room temperature in soft martensitic steels as function of the tempering temperature passes through a maximum, as explained by Folkhard [8]. The austenite formed always increase with tempering temperature above A_{c1}, but after a certain point this high temperature austenite becomes unstable, due to its chemical composition, and partially re-transforms on cooling. On the other hand, double tempered specimens DT-1 and DT-2 showed considerably higher austenite fractions: 0.25 and 0.28, respectively. The first tempering of the double tempering treatment promotes the formation of a high amount of unstable austenite, which partially transforms into martensite on cooling. The A_{c1} temperature of this fresh martensite is lower than 600 °C, due to its high nickel content, and, as a consequence, the second tempering causes the copious precipitation of reversed austenite. Similar behavior was observed by Gesnouin [17] and Bilmes [18] in a supermartensitic steel with 0.5 wt% Mo.

Returning to Fig. 3b, two activation peaks and two reactivation peaks are observed in the DL-EPR curves of double tempered steels. The second and lower peaks are attributed to Ni rich austenite phase [7]. The same behavior was also observed in specimens QT-625 and QT-650 tested with solution 1. The appearance of a second peak in the reactivation scanning suggests that the austenite phase also has Cr-depleted regions. In this study, the calculations of the DOS in double tempered specimens were done with the I_r and I_a currents of the higher peaks.

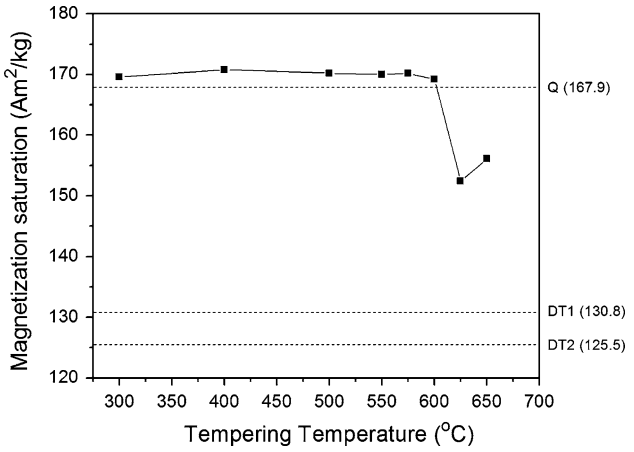

Fig. 8 Variation of magnetization saturation against tempering temperature. Values of specimens Q, DT-1, and DT-2 are also indicated

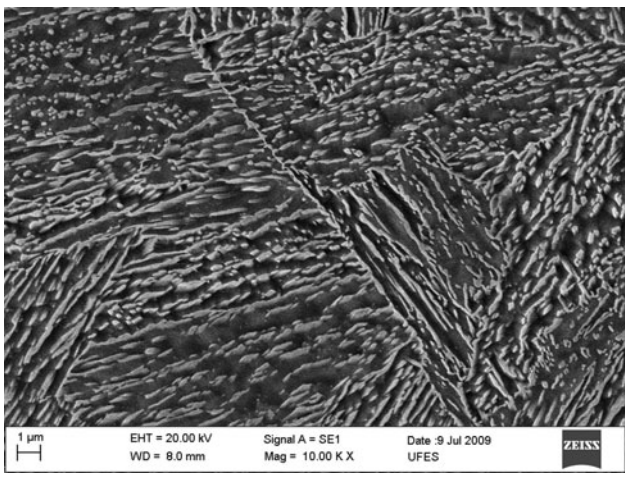

Fig. 9 Microstructure of specimen DT-1

Table 3 Austenite volume fractions (C_γ) determined by magnetization saturation measurements

Specimen	C_γ
Q	0.02
QT-300	<0.01
QT-400	<0.01
QT-500	<0.01
QT-550	<0.01
QT-575	<0.01
QT-600	0.01
QT-625	0.12
QT-650	0.09
DT-1	0.25
DT-2	0.28

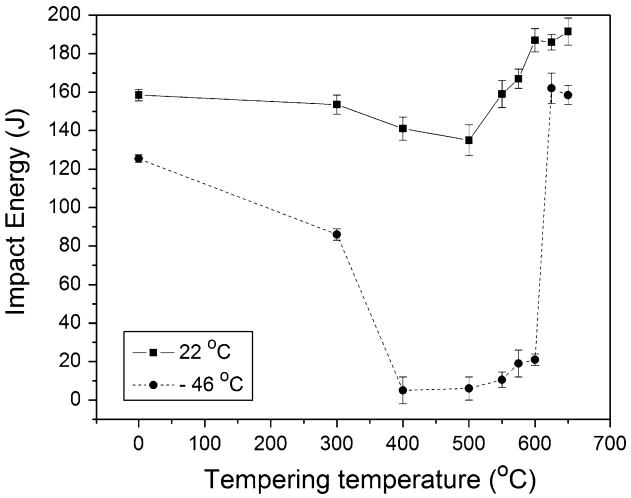

Fig. 10 Variation of the impact toughness with tempering temperature

From previous results in a precipitation hardenable martensitic stainless steel [19], it was expected that an increase of austenite content would increase the toughness, but this was not observed in the room temperature tests of the SMSS analyzed. Specimens DT-1 and DT-2 have impact energy results similar to specimens QT-600, QT-625, and QT-650 (see Table 2; Fig. 4).

The results of low temperature (−46 °C) impact tests are compared to room temperature ones in Fig. 10. The temper embrittlement effect was much more important at −46 °C. Figure 11a–d shows the fracture surfaces of specimens Q, QT-400, QT-600, and QT-625 tested at −46 °C. The as quenched steel presents a ductile behavior with dimples nucleated in square chromium nitrides particles (Fig. 11a) or oxide inclusions (not shown). The specimens QT-400 and QT-600 presented brittle fractures with quasi-cleavage mode and some microcracks (Fig. 11b, c). Specimen QT-625, which was tempered just above the temper embrittlement range, shows a mix of large and small size dimples without quasi-cleavage facets (Fig. 11d).

Specimens double tempered DT-1 and DT-2 tested at −46 °C also showed ductile fractures, with absorbed energy values 146 and 154 J (Table 2), respectively. Similarly to room temperature tests, the increase of austenite fraction with double tempering did not increase the impact toughness in a comparison to specimens single tempered at 625 and 650 °C. This is a somewhat unexpected result, considering the previous works of Bilmes et al. [18] and Nakgawa and Miyazaki [19].

The results presented suggest that specimens double tempered were more susceptible to intergranular corrosion, and have impact toughness similar to specimens single

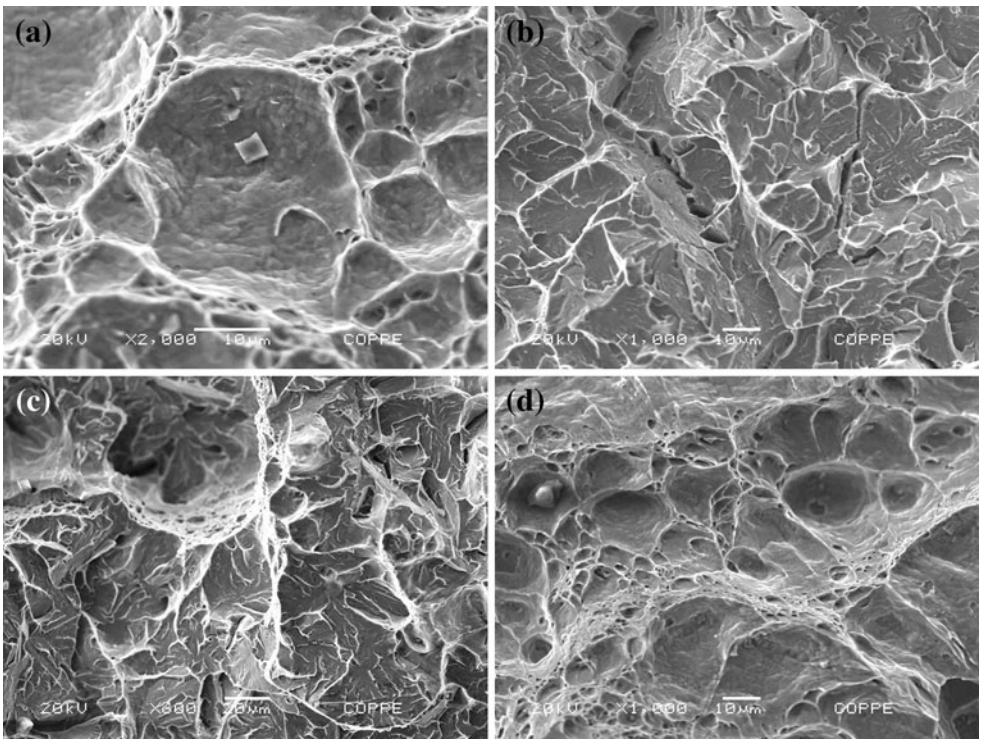

Fig. 11 Fracture analysis of specimens tested at −46 °C: **a** Q; **b** QT-400; **c** QT-600; **d** QT-625

tempered QT-625 and QT-650. On the other hand, as reported by Gesnouin [18], the increase of austenite fraction promoted by double tempering may cause a beneficial decrease in the hydrogen diffusivity, which can increase the resistance to hydrogen embrittlement and stress corrosion cracking.

Some of the results presented and suppositions made in this study must be objects of more detailed investigation in future works. The TiC and Mo_2C precipitations were inferred based on previous works, but were not confirmed by high resolution microscopy. Sensitization detected by DL-EPR tests is due to Cr-depleted areas, and was likely caused by $Cr_{23}C_6$ carbides, since no other Cr-rich phases are previewed in SMSS. Another question that arises from carbides precipitation is the mass balance of carbon. It seems that, although Ti addition was enough to combine with all carbon and nitrogen of the steel, the stabilization was not complete. In austenitic stainless steels (ASS) AISI 321 and 347, for instance, a stabilization heat treatment at around 900 °C must be performed to avoid $Cr_{23}C_6$ precipitation at lower temperatures. Specimens of these steels which are solution treated at 1100 °C become sensitized when re-heated in the 600–700 °C range [20, 21]. Even considering that SMSS steels may have a different behavior from ASS, the examples of AISI 321 and 347 steels show that a theoretical prediction of carbides precipitation is a difficult task because involves thermodynamic and kinetics aspects.

Conclusions

The influence of heat treatments on toughness and sensitization of a Ti-alloyed supermartensitic stainless steel was investigated. The main conclusions of this study are:

- The degree of sensitization increases continuously with the increase of tempering temperature above 400 °C, as measured by DL-EPR tests with 0.25 mol L^{-1} H_2SO_4 + 0.01 mol L^{-1} KSCN solution. Specimen tempered at 650 °C showed a degree of sensitization equal 0.4.
- The estimated A_{c1} temperature of the steel is 607 °C. In agreement, the formation of reversed austenite was detected in specimens tempered at 625 and 650 °C. The austenite volume fractions of these specimens were 0.12 and 0.09, respectively. Double tempering treatments of specimens DT-1 and DT-2 increased the volume fraction of reversed austenite to 0.25 and 0.28, respectively.
- Double tempered specimens DT-1 (670 + 600 °C/2 h) and DT-2 (670 + 600 °C/8 h) showed degrees of sensitization 0.80 and 0.76, respectively. The DL-EPR curves of these specimens showed two activation and two reactivation peaks, which was attributed to the austenite phase.
- The specimens quenched and tempered in all temperatures presented high impact toughness and ductile

behavior in room temperature tests. However, specimens tempered between 400 and 550 °C undergone a slight decrease of impact energy and secondary hardening.

- The temper embrittlement became more evident in the impact tests at −46 °C. Specimens tempered between 400 and 600 °C showed brittle fractures with quasi-cleavage facets and microcracks.
- Despite of the higher austenite volume fraction, the double tempered specimens had impact toughness of the same level of specimens tempered at 625 and 650 °C in tests conducted at 22 and −46°C.

Acknowledgement The authors acknowledge the Brazilian research agencies (CAPES, FAPERJ and CNPq) for financial support.

References

1. Olden V, Thaulow C, Johnsen R (2008) Mater Des 29:1934
2. Kondo K, Ueda M, Oawa K, Amaya H, Hirata H, Takabe H (1999) In: Supermartensitic stainless steels '99', Belgium, p 11
3. Rodrigues CAD, di Lorenzo PL, Sokolowski A, Barbosa CA, Tremiliosi-Filho G, Rollo JMAD (2006) In: 17th Congresso Brasileiro de Engenharia e Ciência dos Materiais, Foz do Iguaçu, p 2695
4. Rodrigues CAD, Lorenzo PLD, Sokolowski A, Barbosa CA, Rollo JMAD (2007) Mater Sci Eng A 460–461:149
5. Pickering FB (1978) Physical metallurgy and the design of steels. Applied Science Publishers Ltd, London
6. ASM (1994) ASM speciality handbook. ASM International, Materials Park
7. Čihal V, Štefec R (2001) Electrochim Acta 46:3867
8. Folkhard E (1984) Welding metallurgy of stainless steels. Springer-Verlag/Wien, New York
9. SM A (1987) ASM metals handbook, vol 12, Fractography. ASM International, Materials Park
10. API Recommended Practice 571 (2003) Damage mechanisms affecting fixed equipment in the refining industry, Section 4: general damage mechanisms—all industries. Americam Petroleum Institute, Washington DC
11. Prohaska M, Kanduth H, Mori G, Grill R, Tischler G (2010) Corros Sci 52(5):1582
12. Lopez N, Cid M, Puiggali M, Azkarate I, Pelayo A (1997) Mater Sci Eng A 229(1–2):123
13. Cullity BD (1978) Elements of X-ray diffraction. Addison Wesley Publishing Company, Reading
14. Leffer B (2010) Stainless steels and their properties. Available in http://www.outokumpu.com/files/Group/HR/Documents/STAINLESS20.pdf. Accessed 27 Nov 2010
15. Tavares SSM, da Silva FJ, Scandian C, da Silva GF, Abreu HFG (2010) Corros Sci 52(11):3835
16. Carrouge D (2011) software MAP_STEEL_AC1TEMP, Phase transformation group, University of Cambridge, Department of Materials Science and Metallurgy. http://www.msm.cam.ac.uk/map/steel/programs/ac1new.html. Accessed 4 Apr 2011
17. Gesnouin C, Hazarabedian A, Bruzzoni P, Ovejero-Garcia J, Bilmes P, Llorente C (2004) Corros Sci 46:1633
18. Bilmes PD, Solari M, Lorente CL (2001) Mater Charact 46:285
19. Nakagawa N, Miyazaki T (1999) J Mater Sci 34:3901. doi:10.1023/A:1004626907367
20. Moura V, Kina AY, Tavares SSM, Lima LD, Mainier FB (2008) J Mater Sci 43:536. doi:10.1007/s10853-007-1785-5
21. Kina AY, Tavares SSM, Souza JA, Abreu HFG (2008) J Mater Process Technol 199:391